

## Biology of Biomechanics:

### *Finite Element Analysis of a Statically Determinate System to Rotate the Occlusal Plane for Correction of Skeletal Class III Openbite Malocclusion*

#### **W. Eugene Roberts, DDS, PhD**

Professor Emeritus of Orthodontics  
Adjunct Professor of Mechanical Engineering  
Indiana University & Purdue University at Indianapolis (IUPUI)  
1121 West Michigan Street, Indianapolis, IN 46202  
317-823-6115, Email [werobert@iu.edu](mailto:werobert@iu.edu)

#### **Rodrigo F. Viecilli, DDS, PhD**

Associate Professor  
Loma Linda University School of Dentistry  
Center for Dental Research, and Department of Orthodontics  
11092 Anderson Street, Loma Linda, CA 92350  
909-558-9498, Email [rviecilli@llu.edu](mailto:rviecilli@llu.edu)

#### **Chris Chang, DDS, PhD**

Founder and Director  
Beethoven Orthodontic Center, and Newton's A, Inc.  
6, Lane 59, Jian-Ghong First Road, Hsinchu, Taiwan,  
Telephone +886 3 5749567,  
Email [Beethoven.tw@gmail.com](mailto:Beethoven.tw@gmail.com)

#### **Thomas R. Katona, DDS, PhD**

Associate Professor  
Orthodontics and Oral Facial Genetics, and Mechanical Engineering  
Indiana University & Purdue University at Indianapolis (IUPUI)  
1121 West Michigan Street, Indianapolis, IN 46202  
317-274-3383, Email [tkatona@iu.edu](mailto:tkatona@iu.edu)

#### **Nasser H. Paydar, PhD**

Chancellor IUPUI, Executive VP, Indiana University  
Professor of Mechanical Engineering, Professor of Informatics and Computing  
301 University Blvd., Suite 5010, Indianapolis, IN 46202, Telephone 317-274-4177, Email [Paydar@iupui.edu](mailto:Paydar@iupui.edu)

**Dedication:** The authors would like to dedicate this article to the memory of Dr. Charles J. Burstone (1928-2015), the father of scientific biomechanics in orthodontics. Although he left Indiana University 45 years ago, he was the mentor of all of us, either directly or indirectly. Rest in peace, Charlie!

## ABSTRACT

**Introduction:** In the absence of adequate animal or *in vitro* models, the biomechanics of human malocclusion must be studied indirectly. Finite element analysis (FEA) is emerging as a clinical technology to assist in diagnosis, treatment planning and retrospective analysis. The hypothesis tested is that instantaneous FEA can approximately predict long-term, mandibular occlusal plane rotation to plan the correction of a skeletal Class III malocclusion.

**Methods:** Seventeen published case reports were selected for patients treated with statically determinate mechanics, utilizing posterior mandible (PM) or infrazygomatic crest (IZC) bone screw anchorage, to retract the lower arch. Two-dimensional (2D) measurements were made for incisor and molar movement, lower arch rotation, and retraction relative to the upper arch. A patient with cone-beam computed tomography (CBCT) imaging was selected for a retrospective finite element analysis (FEA).

**Results:** The mean age ( $\pm$ SD) for the sample was  $23.3\pm 3.3$  years; seven were male and 10 were female. Mean incisor movement was  $3.35\pm 1.55$ mm of retraction and  $2.18\pm 2.51$ mm of extrusion. Corresponding molar movement was retraction of  $4.85\pm 1.78$ mm and intrusion of  $0.85\pm 2.22$ mm. Retraction of the lower arch relative to the upper arch was  $4.88\pm 1.41$ mm. Mean posterior rotation of the lower arch was  $-5.76\pm 4.77^\circ$  (counterclockwise). The mean treatment time ( $n=16$ ) was  $36.2\pm 15.3$  mo. Bone screws in the PM region were more efficient for intruding molars and decreasing the vertical dimension of occlusion (VDO) to close an open bite. The full-cusp, skeletal Class III patient selected for FEA was treated to an ABO CRE score of 24 points in  $\sim 36$ mo by *en masse* retraction and posterior rotation of the mandibular arch: the bilateral load on the lower segment  $\sim 200$ cN. The lower arch was retracted  $\sim 5$ mm, posterior rotation was  $\sim 16.5^\circ$ , and molar intrusion was  $\sim 3$ mm. There was a  $4^\circ$  decrease in the mandibular plane angle (MPA) to close the skeletal openbite. Retrospective sequential iterations (FEA animation) simulated the clinical response, as documented with longitudinal cephalometrics. The level of PDL stress was relatively uniform ( $<5$ kPa) for all teeth in the lower arch segment.

**Conclusions:** *En masse* retraction of the lower arch is efficient for conservatively treating skeletal Class III malocclusion. PM anchorage results in intrusion of molars to close the VDO and MPA. Instantaneous FEA as modeled here could be used to reasonably predict the clinical results of an applied load.

Key Words: extra-alveolar orthodontic anchorage, finite element analysis, root resorption, material properties of archwires, non-extraction treatment, skeletal malocclusion, PDL stress, *en masse* tooth movement

## Introduction

In orthodontics, the term “biomechanics” is often restricted to the physics of *mechanics*.<sup>1</sup> Forces and moments can be calculated in three dimensions (3D) for statically *determinate* mechanics: those that can be calculated using the principles of static equilibrium (Newton’s Laws) (Fig. 1). However, **biomechanics** is actually the science of how applied loads affect **biologic** structures, such as the supporting periodontium (Fig. 2). Rather than relating to the center of mass, as for a tooth in space (Fig. 1), the response to an applied force is relative to the center of resistance (Cres) of the supported root (Fig. 2). Forces and moments can be measured or calculated for individual teeth along an archwire,<sup>2,3</sup> but the boundary conditions, such as bracket engagement, effects of adjacent teeth, and the variance of the load delivered over time, are difficult to control. Typical archwires deliver unknown loads to the supporting tissues in an undefined manner: *the biologic black box*. Unfortunately, there are no appropriate bench or animal models for comprehensive clinical orthodontics. Realistic studies must be performed on clinical records of specific patients.<sup>4</sup>

The objective of this report is to assess a novel clinical method for conservative treatment of skeletal malocclusion, and evaluate the biomechanical predictability of the clinical response at the PDL level, with advanced engineering technology. Since this report is intended for *clinicians*, a succinct review of some fundamental principles of mechanical engineering, relative to the unique material properties of the PDL and other supporting tissues, is required to convey the clinical significance of finite element analysis (FEA) reported.

## Defining Terms

- **Tension, compression, shear** and **torsion** are illustrated in Figure 3.
- **Tensors** are a continuous mathematical framework in physics. **Scalars** are at one end of the scale: zero order tensors with magnitudes but no directionality. **Vectors**, first order tensors, possess magnitude and direction (Fig. 4A). In addition, a *force* vector has a point of application, and a line of action. Within a structure is loaded, external loads (forces and moments) are expressed as stresses (second order tensors)(Fig. 4B). Stress is a higher order term than a vector (force) because it is more complex (force/unit area). The mechanical properties of the more complex (higher order) tensors provide the mathematical relationships between stresses and strains. For instance, Young’s modulus of elasticity (material stiffness) and Poisson’s ratio (ratio of deformation, in the perpendicular dimension, as a material is stretched or compressed in the axial direction) are fourth order tensors (Fig. 3). In the most general state, the number of independent stresses is reduced to 6 (Fig. 4C). Fortunately, with respect to controlling the complexity of calculations, there is an orientation where the shear stresses equal zero, and then the associate normal stresses are referred to a principal stresses ( $\sigma_n$ ).  $\sigma_1$  is maximal,  $\sigma_2$  is intermediate, and  $\sigma_3$  is minimal principal stress. All of the

PSs may be in compression or tension, but  $\sigma_1$  is the “most” tensile (or least compressive), and  $\sigma_3$  is the “most” compressive (or least tensile).  $\sigma_3$  is particularly important in orthodontics because it is directly related to PDL necrosis and the path of tooth movement.<sup>5-7</sup> A common but less mathematically precise designation for  $\sigma_1$ ,  $\sigma_2$  and  $\sigma_3$  is P1, P2, and P3, respectively (Fig. 4D).

- **Force** is an interaction that tends to change the motion of an object, or in the current context, forces deform structures. It is a vector with direction, magnitude, line of action and frequency (if intermittent). Its unit is Newton (N)  $\sim 102g @ 1G$  (Earth’s gravity).<sup>4,8</sup>
- **Stress** is the internal force per unit area, and its unit of measure is a Pascal (Pa):  $1N/meter^2$ . As previously explained, stress is a second order tensor with 6 independent components, representing the normal and shear stresses in each plane (Fig. 4B). A Pa is a very small value, so most relevant physiologic stresses are expressed in kilo (k), mega (M) or giga (G) Pascals, which are  $10^3$ ,  $10^6$  or  $10^9$ , respectively.<sup>9-11</sup>
- **Pressure** is a scalar quantity, so the stresses (compressive or tensile) are the same in all directions (isotropic).
- **Strain** is deformation per unit length. The term itself is *dimensionless* because it is a relative reference, similar to percentage. For example, a 100mm length of bone flexed (bent) or elongated 1mm, is exposed to 1% deformation or 0.01 strain. Bone will typically fracture when bent  $\sim 2.5\%$ , so a full “unit” of strain ( $\epsilon$ ) is a very large distortion, that considerably exceeds the ultimate strength of bone. It follows that the physiologic influence of strain on a living bone is at the microstrain ( $\mu\epsilon$ ) level, which is  $10^{-6}$  strain or  $10,000 \mu\epsilon$ . Frost’s mechanostat (Fig. 5) summarizes the differential bone response to varying levels of strain.<sup>4</sup>
- **Finite Element Analysis (FEA)** is a numerical method (Fig. 6) for calculating the levels of stress in a homogeneous or composite structure, based on the **material properties** of each of its components.<sup>5,6</sup>

**Statically Determinate Mechanics:** The term “*biomechanics*” is usually applied to the static equilibrium of applied loads, but *statically determinate* mechanics are typically restricted to simple collinear forces or two parallel force-one couple 2D systems. For 3D statically determinate systems, there can be 3 force components and 3 moment components. In the absence of true 3D mechanics, orthodontists typically apply 2D mechanics in the sagittal and frontal planes, but that approach falls short of a true 3D statically determinate system. Movement of multiple teeth with a flexible archwire is indeterminate (Figs. 7A & B), but *en masse* movement of an entire dental arch as a segment may be determinate (Fig. 8), if there is negligible change in the relative position of individual teeth as the segment is moved. A rigid wire completely filling the slot on every tooth is *not* required, but the archwire must provide sufficient torque control to prevent changes in the axial inclination of teeth in the segment.

Accurate determination of the applied load is critical for reliably calculating stress in supporting structures. Unfortunately, appliances conforming to the restraints of statics and equilibrium are rare in the clinic, because the term “determinate mechanics” is typically applicable to two teeth or dental segments.<sup>7</sup> A common “exception” is the symmetrical molar anchorage for an intrusive base-arch. These mechanics are *determinate* for the incisors and bilateral molars, if there is no cinch-back;<sup>8</sup> however, some form of tie-back or other less predictable restraint such as friction also occurs. It follows that most clinical mechanics are indeterminate, including typical archwires, engaged in multiple brackets. Reliable FEA to determine PDL stress requires known (determinate) loads that are reasonably constant. On the other hand, indeterminate mechanics can be effective for precise alignment of teeth (Figs. 7A & B), but that approach is typically less predictable because the load delivered to the supporting tissues is unknown. Measuring moments and forces at the archwire level may be helpful for understanding the loads applied,<sup>2,3</sup> but extrapolation to stress levels in the PDL is uncertain, unless all of the boundary conditions are controlled.

**Mechanical Properties:** The “memory shape” of flexible archwires is the basis for most fixed appliance therapy. This indeterminate approach (Figs. 7A & B) may be effective, but it can (and often does) produce “a clinical surprise.”<sup>1</sup> If a deformed archwire is not physically altered, it tends to recover its original conformation but at an unknown 3D planar orientation, delivering constantly changing loads to periodontium over time. In effect, the teeth align “to the archwire” in an unpredictable manner, and as Dr. Charles Burstone<sup>1</sup> so aptly concluded: “The wire does the thinking!” He subsequently developed the *segmented arch technique* to take advantage of determinate systems for *en masse* tooth movement.<sup>1</sup> He later preferred to refer to his principles as “scientific biomechanics”, because, most “techniques” are a cookbook approach. The segmented arch approach utilizes scientific principles that are universal, and not unique to orthodontics. Burstone’s determinate mechanics<sup>1</sup> is the basis for the present FEA.

**Periodontal Ligament:** The thin soft tissue interface, between the root of a tooth and its supporting bone, is a stress riser with a relatively low modulus of elasticity (stiffness). It serves as a biologic transducer for osseous adaptation, permitting a tooth to move relative to its apical base of bone.<sup>4</sup> The viscoelastic component of PDL displacement has been modeled in vitro,<sup>5</sup> but the vascular reflex to resist compression has only been documented in animals.<sup>4</sup> It is widely assumed that all continuous orthodontic loads result in at least some transient PDL necrosis, the “lag-phase of tooth movement,”<sup>4,8</sup> but the PDL-level biomechanics for *en masse* tooth movement have never been rigorously tested. Assuming the dental load is known (determinate or reliably measured), a FEA can calculate the stress throughout the supporting structures, including the PDL. The critical factor in eliciting desirable tooth movement is the *level of stress* in the PDL. In rodents, stress >8-10kPa usually compresses PDL to the point of necrosis, thereby at least transiently inhibiting tooth movement.<sup>4,8,10</sup> PDL necrosis is also associated with the expression of root resorption.<sup>8,10</sup> In these studies, the data show that PDL stress <8kPa is *optimal*

because it induces and maintains bone modeling reactions (formation and resorption) in the plane of tooth movement, without necrosis and increased risk of root resorption. These rodent data are intriguing, but require confirmation in humans.

PDL is a unique tissue with a variable modulus of elasticity, due to its viscoelastic properties and characteristic vascular response, which transiently resists compression in support of masticatory function.<sup>4</sup> It is challenging to model the PDL with FEA because it does not have a fixed modulus of elasticity. Fortunately this has not been a major problem, probably because the PDL modulus is so much less than those of the adjacent rigid structures (tooth and bone). Little change is noted in the overall FEA results for even an order of magnitude variance in the PDL modulus.<sup>7</sup> However, there is still a significant limitation for calculating stress in the PDL. It can only be an approximation, so PDL stress results should be consistent with experimental or clinical data.<sup>8-10</sup>

The objective of this report is to use FEA to retrospectively assess mandibular arch retraction and posterior rotation, to correct Class III openbite malocclusion.

## **Materials and Methods**

A PubMed advanced search of the literature was performed in September, 2015, with three search items: 1. Skeletal Class III malocclusion, 2. Bone screws, and 3. Nonsurgical treatment. One case report was recovered: Jing et al. 2013.<sup>12</sup> The entire mandibular arch of a 20 yr old female, with a skeletal Class III malocclusion, was retracted 4mm. The anchorage was provided by a miniscrews, placed in the external oblique ridges of the mandible. Progressive, flexible CuNiTi archwires were used in the lower arch while it was retracted, so the mechanics were *indeterminate*.

Two unpublished, skeletal Class III case reports were sourced from the records of one of the authors (CHC) to distinguish *indeterminate* (Figs. 7A and B) from *determinate* (Fig. 8) mechanics. The statics for both force systems appear similar, but there are several critical factors for achieving *determinate* mechanics, that are amenable to the FEA: 1. Full-size archwire (engaging anterior torque) in the lower arch during the entire retraction phase constitutes a segment, 2. Relatively constant force of superelastic NiTi springs can be effectively modeled over time, and 3. The force is applied directly to the archwire (Fig. 8). For the present study, the concept of a “segment” in the sagittal plane was defined as a block of teeth with a “full-size archwire,” which means it engaged torque in the brackets on the anterior teeth, so that the entire arch was retracted *en masse* with no significant dental tipping. In general, any variance from a segment with the retracting force acting on the archwire results in indeterminate mechanics. When the retracting force is applied to a tooth (Fig. 7), there is a tendency for it to rotate (Fig. 2), introducing an uncontrolled variable. If progressive archwires are applied as the arch is retracted, there is individual movement of teeth, which violates the concept of a segment.

Seventeen Class III patients treated with *determinate* mechanics were sampled online. Superelastic NiTi springs, anchored with extra-alveolar (E-A) bone screws, delivered ~200-300kN of force bilaterally to retract and rotate the entire lower arch as a segment. The case reports were published in *News & Trends in Orthodontics* 2008-10, and the *International Journal of Orthodontics and Implantology* 2011-15 (<http://iaoi.pro/archive/journal>). The published cephalometric films and intraoral photographs were downloaded. Some incomplete or low magnification illustrations were supplemented with original records, that were submitted to the publisher by the authors. Magnification of downloaded records was controlled, by adjusting the width of the mandibular first molar to 11.0mm.<sup>13</sup> Lower arch retraction was measured in 2D as incisal and molar movement in the sagittal and vertical dimensions, and the direction of lower arch rotation was determined in degrees. Positive values were assigned to extrusion and protrusion of teeth, while negative values were recorded for intrusion and protraction. Clockwise rotation was positive, and counterclockwise was negative. The age and sex of all the patients was recorded. Ten patients in the series were scored with the American Board of Orthodontics (ABO) Discrepancy Index (DI) and Cast-Radiograph Evaluation (CRE). Six of the patients also had an International Association of Orthodontics and Implantology (IAOI) Pink & White (P&W)(Su 2012) dental esthetics score, which is a modification of the method of Belser et al.<sup>15</sup>

One male patient treated for skeletal Class III openbite malocclusion from age 21-24yr was of special interest because: 1. Pretreatment cephalometric records were collected for the last three years of aberrant growth (18-21yr) to help establish the etiology of the malocclusion (Fig. 9), 2. Two different directions of force, from either the infrazygomatic crest (IZC) or posterior mandible (PM), were used at separate times for lower arch retraction (Figs. 10), 3. The inferior direction of traction (PM) was superior to the IZC anchorage site for closing the openbite by intruding lower molars to decrease the VDO, and 4. CBCT imaging was available for FEA.<sup>16</sup> The fixed appliance was composed of Damon Q® passive self-ligating brackets (Ormco, Glendora, CA). According to the manufacturers prescription, standard torque brackets were used on all teeth except for the lower left canine, which was bonded with a high torque bracket. The archwire sequence progressed to 0.019x0.025" stainless steel, prior to lower arch retraction.<sup>16</sup> The retraction force was 200cN via a superelastic NiTi closed coil, that was transiently supplemented with a triangular tie of elastic thread encircling the canine, distal molar and PM bone screw. The load from the latter was expected to be relatively small and decay rapidly. All considered, the retraction force for the FEA was modeled as ~200cN of constant force, applied to the archwire mesial to the canine, bilaterally. Then the FEA was compared with the clinical results (Figs. 11 and 12).

### **Finite Element Modeling**

The patient was modeled by scaling a standard template of 3D teeth and supporting bone to the specific tooth dimensions obtained with the CBCT scan.<sup>16</sup> The PDL was constructed using dilation and intersection operations in Simpleware® (Exeter, UK),

with a uniform width of 0.2mm. Standard homogeneous linear material properties, that are commonly used in the literature, were assigned (Tooth=20GPa, Bone=12GPa and PDL= 0.5 MPa)<sup>6,9,10</sup> Subsequently, the model was meshed and exported into the ANSYS Mechanical APDL® finite element program (Canonsburg PA). The mesh consisted of quadratic tetrahedrons, with nodes shared at the material interfaces, and it approximated 1.2 million elements. The mandibular bone was fixed, and the teeth were loaded utilizing the approximate load direction and magnitude applied to the patient as published.<sup>16</sup> To model tooth movement of the occlusal plane in the long term, rather than individual tooth movements, the teeth were connected with enamel through the interproximal contacts. This was done to simulate a long-term effect, because even with a stiff archwire the teeth will initially move individually until equilibrium is achieved after archwire deformation. Connecting the teeth rigidly at the interproximal level circumvents this difficulty, because realistic modeling would overvalue individual tooth movements compared to occlusal plane movement. Furthermore, retrospective cephalometrics documented that the lower arch was moved as a segment (Fig. 12). The instantaneous displacement and PDL stresses (iterations) were acquired from the solution to compare instantaneous displacement with animation to compare to the long-term dental and orthopedic response (Figs. 11 and 12). The equipment used for this clinically relevant simulation and analysis was a Hewlett-Packard (Palo Alto, CA) HP830 workstation with 16 cores at 3.2ghz, and 64gb of ram. A k20 tesla card and a 512k solid-state hard-drive were used to decrease the processing time. The FEA reported here required less than five minutes, with a computer that can sit on a desktop.

## Results

The mean age was  $23.3 \pm 3.3$  years for the 17 skeletal Class III patients sampled. Seven were male and 10 were female. Table 1 presents the data (mean $\pm$ SD) for 2D movement of molars and incisors, rotation of the lower arch, treatment time, and for the clinical outcomes that were provided.

The finite element program calculated the axis of rotation (Fig. 13) for mandibular arch retraction, and then documented the change in tooth positions from start to finish (Fig. 14). Finite element animation demonstrated that the rotation of the lower arch resulted in molar intrusion of  $\sim 3$ mm, to reduce the VDO and close the mandibular plane angle (Figs. 11 and 14). The openbite was closed by forward rotation of the mandible, and  $\sim 2$ mm extrusion of the incisors, due to posterior rotation of the lower arch segment (Figs. 11, 12 and 14). Finite element calculation of the third (most compressive) principal stress ( $\sigma_3$ ) revealed a relatively uniform level of stress in the PDL  $< 5$ kPa for all teeth, but this is only an approximation (Fig. 15).



## Discussion

The 18 published case reports reviewed for this study revealed that 17 of the patients were treated with statically determinate mechanics for en masse retraction of the lower arch. For the latter sample, the line of force for retracting the mandibular segment varied according to the site of the bone screws: PM or IZC (Fig. 10). For the purposes of this study, the mechanics for PM anchorage with miniscrews is identical to that for MBS bone screws. Intrusion of lower molars to decrease facial height (Figs. 11 and 13) was associated with bone screws placed in the PM, but not in the (IZC)(Fig. 10).<sup>16</sup> Both anchorage screw locations produced about the same distal force, but PM anchorage generated less counterclockwise moment, and delivered a modest intrusive force (Fig. 10). The theoretical load diagram for PM anchorage was confirmed with FEA (Figs. 12 and 13), and the actual clinical results (Figs. 11 and 12). These data demonstrate that a severe Class III openbite malocclusion can be treated conservatively, without extractions or orthognathic surgery, by reversing the etiology of the malocclusion, which was anterior rotation of the lower arch. Posterior rotation of the mandibular arch reversed the etiology of the malocclusion, thereby simultaneously decreasing the mandibular plane angle, vertical dimension of occlusion, and openbite (Fig. 11).<sup>16</sup>

The patient selected for FEA experienced molar intrusion and a decrease in facial height when the lower arch was retracted with PM anchorage (Figs. 8 and 10). The openbite continued to close when a retraction force was anchored in the IZC region (Fig. 7B), but there was no further improvement in the VDO.<sup>16</sup> In effect, the more inferior direction of traction (Figs. 8 and 10) reversed the etiology of the openbite malocclusion, as documented with pretreatment cephalometrics from 18-21 yrs (Fig. 9), and decreased both the openbite and facial height to achieve lip competence (Fig. 11).

The published case selected for the FEA had a unique scenario. The initial mandibular buccal shelf (MBS) bone screws failed because they were placed deep in the buccal fold.<sup>16</sup> Despite an apically repositioned flap of attached gingiva, soft tissue irritation prevented their use for anchorage. The MBS bone screws were removed, and interradicular miniscrews (IRMS) were placed distal to the roots of the first molars. The latter provided approximately the same PM anchorage as MBS bone screws (Fig. 10), but they could potentially block the path of tooth movement. Indeed, the roots of the lower first molars did contact the IRMS after ~14 months of mandibular retraction. The lower IRMS were removed and IZC bone screws were placed in the posterior maxilla to continue lower arch retraction and close the anterior openbite. Fortunately, a CBCT image was obtained to assess root contact with the IRMS, so that 3D radiographic image marked the end of PM and the start of posterior maxillary (IZC) anchorage (Fig. 10). That scenario produced the opportunity to compare lower arch retraction with PM or IZC anchorage.<sup>16</sup> Since the CBCT image was available, it was then possible to study the most favorable mechanics with FEA.

Recently, the soft tissue irritation problem for MBS bone screws has been solved by placing longer screws that have at least 5mm of clearance between the soft tissue insertion point and the head of the screw.<sup>17</sup> With the latter method, there was no significant difference in the success rate for >1600 MBS bone screws, placed in either attached gingiva or moveable mucosa. Unfortunately, there are no CBCT records for the other case reports reviewed (n=16), so they cannot be analyzed with the current FEA method. As CBCT imaging becomes more routine in clinical practice, FEA is a promising approach for testing different types of force systems.

### **Conclusions**

Skeletal Class III malocclusion was conservatively corrected (without extractions or orthognathic surgery) by applying statically determinate mechanics to retract the entire mandibular arch. In <5 minutes, a desktop computer simulated the efficient clinical result with FEA animation, and estimated the level of PDL stress, associated with the applied mechanics. As orthodontics and dentofacial orthopedics enters the 3D age, this method can be used to design efficient mechanics, with a low risk of root resorption, for the conservative management of malocclusion.

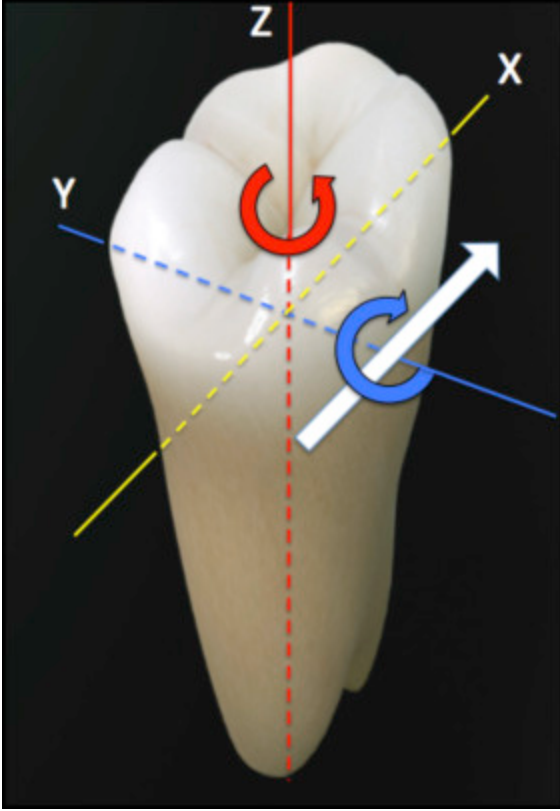
### **Acknowledgements**

This research is a the product of a 25 year cooperative effort at Indiana University & Purdue University at Indianapolis (IUPUI), between the Purdue School of Engineering & Technology, and the Indiana University School of Dentistry. The authors acknowledge the insightful leadership of Chancellor Gerald Bepko, Dental Dean H. William Gilmore, and Engineering Dean Bruce Renda in creating this interactive biomechanics program in 1990. Dr. John J-J Lin, Dr. Irene Shih and Ms Bella Chu provided original records as needed for the published case (reference 16). Professor Jie Chen provided valuable advice for the preparation of the manuscript.

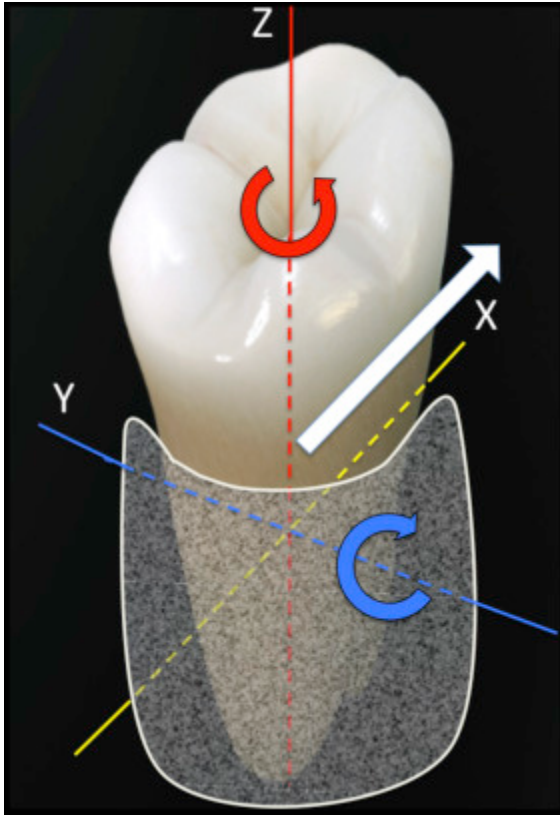
### **References Cited**

1. Burstone CJ. Physics and clinical orthodontics: 100 years ago and today. *Am J Orthod Dentofacial Orthop.* 2015;147:293-294.
2. Badawi HM, Toogood RW, Carey JPR, Heo G, Major PW. Three dimensional orthodontic force measurements. *Am J Orthod Dentofacial Orthop.* 2009;136:518-528.
3. Major PW, Toogood RW, Badawi HM, Carey JP, Seru S. Effect of wire size on maxillary arch force/couple systems for a simulated high canine impaction. *J Orthod.* 2014;41:285-291.
4. Roberts WE. Bone physiology, metabolism and biomechanics in orthodontic practice. Chapter 10 In: Graber LW, Vanarsdall Jr RL, Vig KWL, editors: *Orthodontics Current Principles and Techniques*, 5<sup>th</sup> ed. St. Louis: Elsevier Mosby; 2012, pp 287-343.

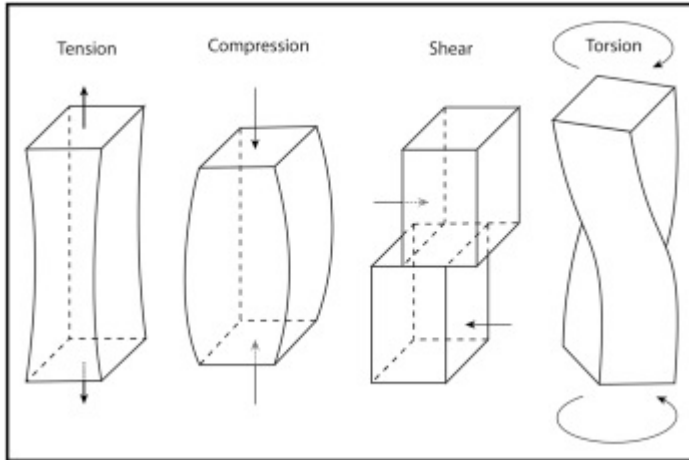
5. Xia Z, Chen J. Biomechanical validation of an artificial tooth-periodontal ligament-bone complex for in vitro orthodontic load measurement. *Angle Orthod.* 2013;83:410-417.
6. Paydar, N., Akay, H.U., Poyraz, C.L. and Roberts, W.E. Finite element model of a human mandible for investigating joint reactions and bone stresses during mastication. *Proceedings of the ASME Winter Annual Meeting, Bioengineering Division, Atlanta, GA. December 1-6, 1991, BED Vol. 20, Advances in Bioengineering*, pp. 163-166.
7. Katona TR, Paydar NH, Akay HU, Roberts WE. Stress analysis of bone modeling response to rat molar orthodontics. *J Biomechanics* 1995;28(1):27-38.
8. Proffit WR, Fields HW Jr, Sarver DM. *Contemporary orthodontics*, 4th Ed., Mosby-Elsevier, St. Louis, 2007, pp383-385.
9. Viecilli RF, Katona TR, Chen J, Hartsfield Jr JK, Roberts WE. Three-dimensional mechanical environment of orthodontics tooth movement and root resorption. *Am J Orthod Dentofacial Orthop.* 2008;133(6):791.e11-26.
10. Viecilli RF, Kar-Kuri MH, Varriale J, Budiman A, Janal M. Effects of initial stresses and time on orthodontic external root resorption. *J Dent Res.* 2013;92(4):346-51.
11. Van Schepdael A, Geris L, Vander Sloten J. Analytical determination of stress patterns in the periodontal ligament during orthodontic tooth movement. *Med Eng Phys.* 2013;35(3):403-410.
12. Jing Y, Han X, Guo Y, Bai D. Nonsurgical correction of a Class III malocclusion in an adult with miniscrew-assisted mandibular dentition distalization. *Am J Orthod Dentofacial Orthop.* 2013;143(6):877-887.
13. Manchanda AS, Narang RS, Kashion SS, Singh B. Diagonal tooth measurements is sex assessment: A study on North Indian population. *J Forensic Dent Sci.* 2015;7(2):126-31.
14. Su B. IBOI pink & white esthetic score. *International Journal of Orthodontics & Implantology* 2012;28:80-85.
15. Belser UC, Grutter L, Vailati F, Bornstein MM, Weber HP, Buser D (2009). "Outcome evaluation of early placed maxillary anterior single-tooth implants using objective esthetic criteria: a cross-sectional, retrospective study in 45 patients with a 2- to 4-year follow-up using pink and white esthetic scores." *J Periodontol* **80**(1): 140-151.
16. Shih I Y-H, Lin J J-J, Roberts WE. Conservative correction of severe class III open bite: 3 force vectors to reverse the dysplasia by retracting and rotating the entire lower arch. *International Journal of Orthodontics & Implantology* 2015;38:4-18. Available online: <http://iaoi.pro/archive/post/id/169>
17. Chang C, Liu Sean S-Y, Roberts WE. Primary failure rate for 1680 extra-alveolar mandibular buccal shelf miniscrews placed in movable mucosa or attached gingiva. *Angle Orthod.* (In Press, published online Jan 20, 2015).



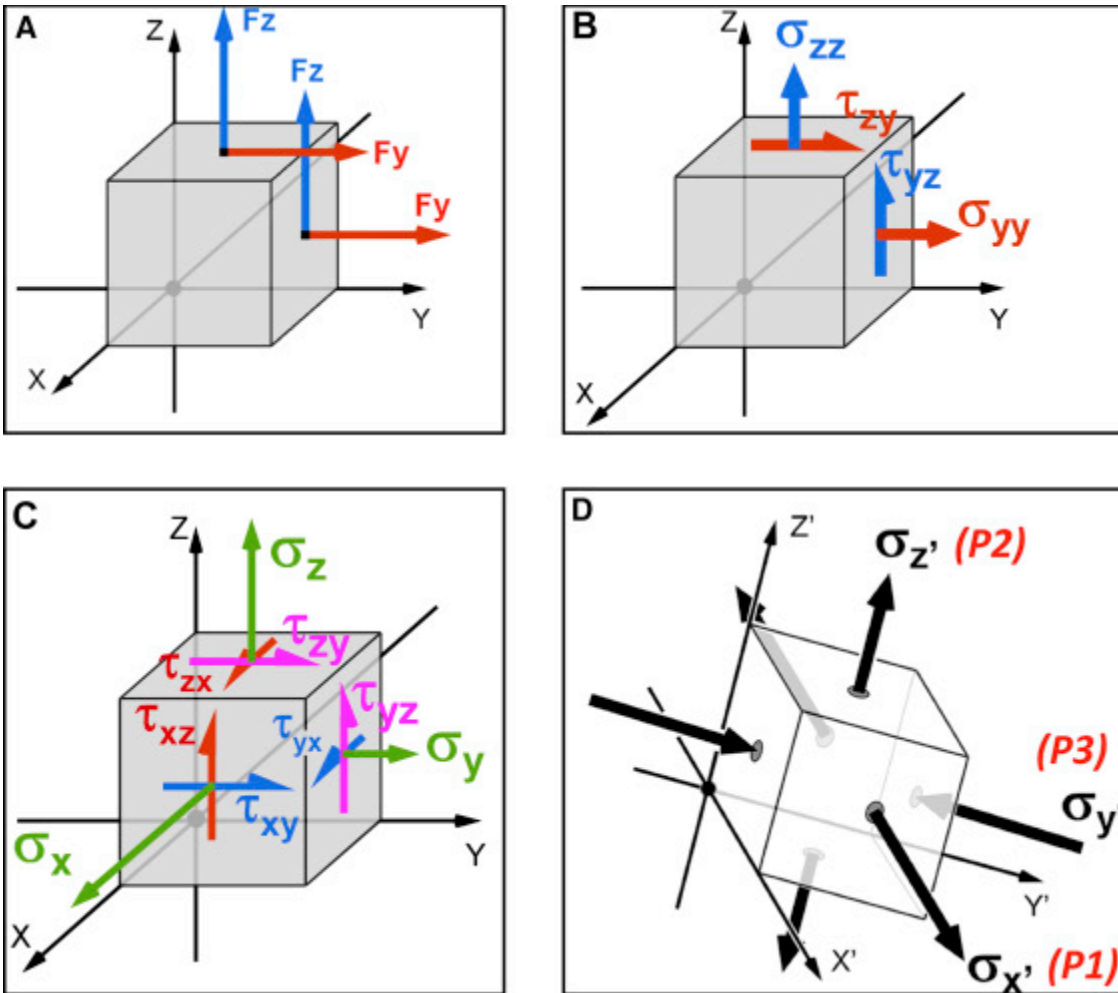
1. A force (white arrow), applied at the buccal surface of a lower molar in space, produces moments in the axial (red) and sagittal (blue) planes, relative to the center of mass for the tooth (intersection of the X, Y and Z planes).



2. When the tooth is restrained by bone (white texture overlay), the same force (Fig. 1) results in a complex biologic response in 3D, relative to the center of resistance ( $C_{res}$ ), which is the intersection of the X, Y and Z planes. Note that this “restrained body effect” displaces the Y axis for tipping in the sagittal plane (X) to the  $C_{res}$ , which is about 1/3 of the distance from the alveolar crest to the apex of the tooth. The tooth simultaneously tips around the Y axis and rotates around the Z axis in response to a force (white arrow) applied at the buccal surface. Little is known about the biomechanics of the tissue response, so that is deemed the “biologic black box.”



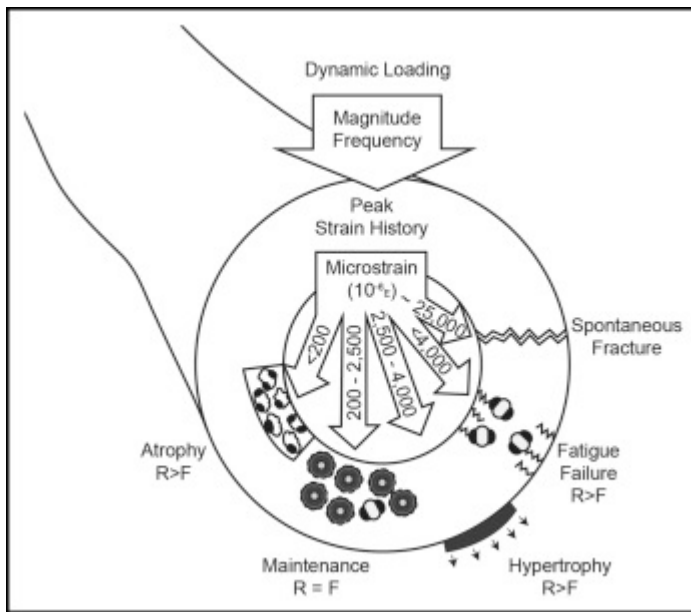
3. In mechanics there are four fundamental loads, which elicit a distinct response in a loaded material: tension, compression, shear and torsion. According to Poisson's ratio, loading in tension and compression results in narrowing or widening the loaded structure as its length changes. See text for details.



- 4      **A.** An imaginary, infinitesimally small cube, cut-out from within any loaded structure (beams, trusses, bone, PDL, root, . . . ), experiences internal forces. Two such force components are shown acting on 2 of the 6 cube faces. On the top surface,  $F_z$  is the “normal” (perpendicular) force.  $F_y$  is a “shear” force because it acts within that plane. On the right surface,  $F_y$  becomes the normal force, and  $F_z$  becomes a shear force. Similar relationships apply to the other 4 faces of the cube. The  $F_z$  and  $F_y$  forces are shown in tension (arrow pointing away from the surface), but they can also be in compression (arrow pointing into the surface).
- B.** When a force component is divided by the area of the surface on which it acts, it becomes a stress component (second order tensor). The 1<sup>st</sup> subscript indicates the direction of the stress component and the 2<sup>nd</sup> subscript designates the cube face on which it acts. Thus, the normal stresses are typically denoted as  $\sigma_{xx}$ ,  $\sigma_{yy}$  and  $\sigma_{zz}$ , but they may be expressed as  $\sigma_x$ ,  $\sigma_y$  and  $\sigma_z$  without the redundancy of the double subscripts. Compressive normal stresses are *negative* while tensile stresses are *positive*. The shear stresses are generally written as  $\tau_{xy}$ ,  $\tau_{xz}$ ,  $\tau_{yz}$ ,  $\tau_{yx}$ ,  $\tau_{zx}$ , and  $\tau_{zy}$ . Again the drawing is only showing two planes, but the same relationship applies to the other four faces of the cube.

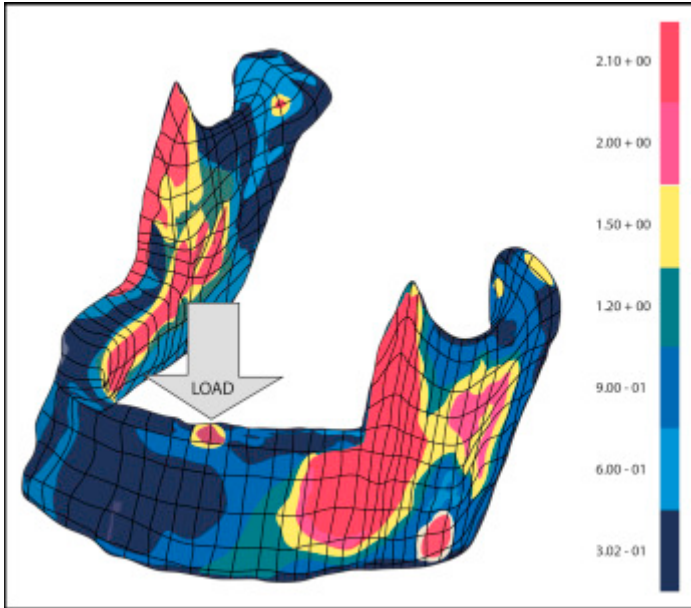
C. The most general state of stress is illustrated for 3 faces of the cube. Equilibrium dictates that some (opposing) stresses are equal, so  $\tau_{xy} = \tau_{yx}$ ,  $\tau_{xz} = \tau_{zx}$ , and  $\tau_{yz} = \tau_{zy}$ , thus reducing the number of independent stresses to 6.

D. It is possible to calculate an orientation of the imaginary cube where all of the shear stresses equal 0. That orientation is the principal direction (X'-Y'-Z') and the associated normal stresses are the principal stresses,  $\sigma_{x'}$ ,  $\sigma_{y'}$  and  $\sigma_{z'}$ . All the principal stresses can be in compression or tension, but the relative order is fixed. The “most” tensile (least compressive) of the 3 ( $\sigma_{x'}$ , as drawn) is the maximum principal stress, which is designated as P1. The “most” compressive (least tensile) ( $\sigma_{y'}$ ) is P3, the minimum principal stress. The second principal stress, P2, is in-between ( $\sigma_{z'}$ ).

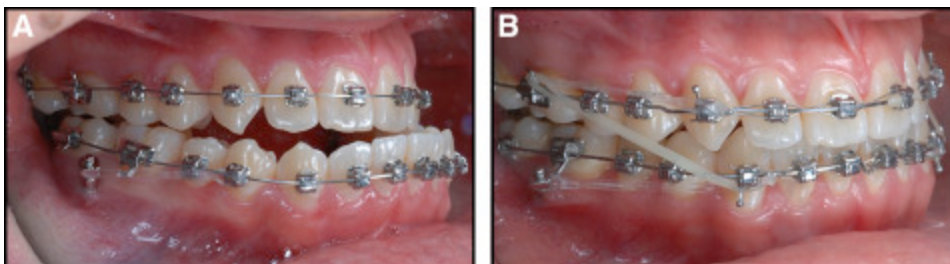


5. Frost's Mechanostat describes the relationship of bone strain to the progressive hierarchy of bone atrophy, maintenance, hypertrophy, fatigue failure, and spontaneous fracture. The relative effects on bone resorption (R) and formation (F) are illustrated. See text for details.



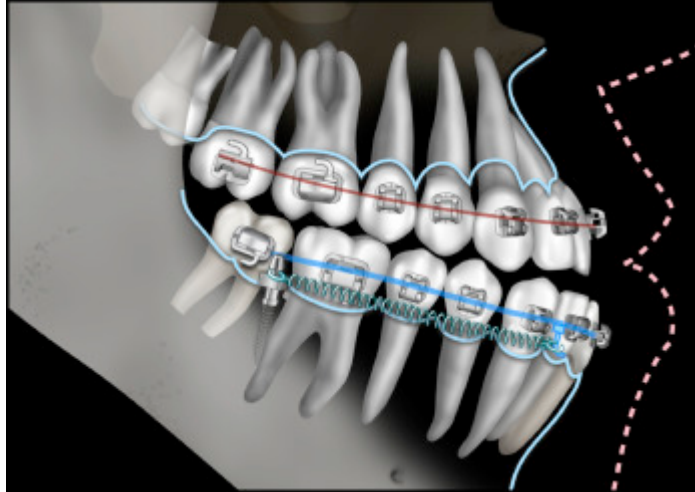


6. A color illustration of an early finite element model of the human mandible, originally published in black and white, shows the stress distribution in MPa, relative to a 1N load applied to the left first premolar area (arrow). The mandible is a cantilever exposed to substantial bending and torsion, particularly in the posterior body, mandibular ramus, and coronoid process, as designated by the yellow, orange and red areas. See Paydar et al. (reference 6) for details.

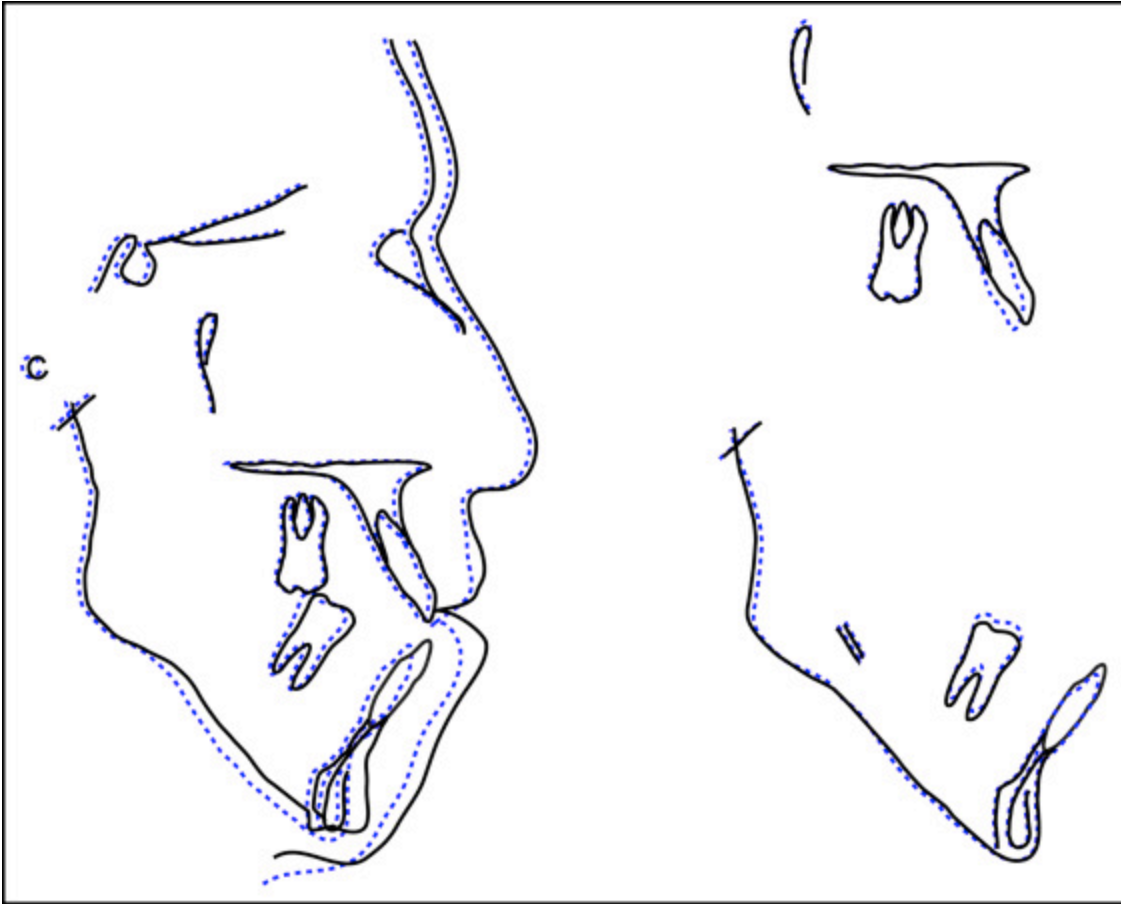


7. **A.** Indeterminate mechanics, an elastomeric chain anchored with mandibular buccal shelf (MBS) bone screws bilaterally, are illustrated for correction of skeletal Class III malocclusion, with traction beginning at 9mo into treatment.

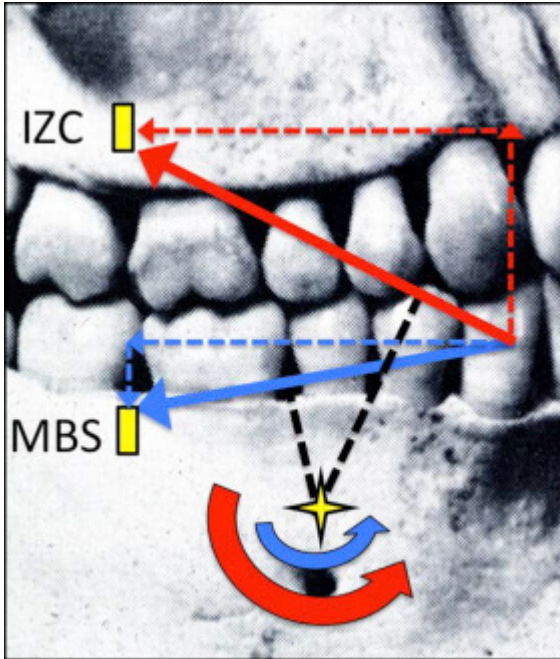
**B.** At 20mo into treatment (11mo later) the mechanics are effective but indeterminate, so they cannot be reliably modeled with the current FEA method. See text for details.



8. Determinate mechanics are produced by  $\sim 200\text{cN}$  of superelastic NiTi force generated from MBS bone screws. The force is applied bilaterally to a full-size archwire. Under these conditions, the lower arch is a segment. This 3D graphic is a revised original illustration by Dr. Rungsi Thaharungkul.



9. Cephalometrics documents the pretreatment growth of a male from 18yr (black) to 21 yr (dashed blue) of age. The progress tracing is dashed because there was no active treatment from 18-21yr.



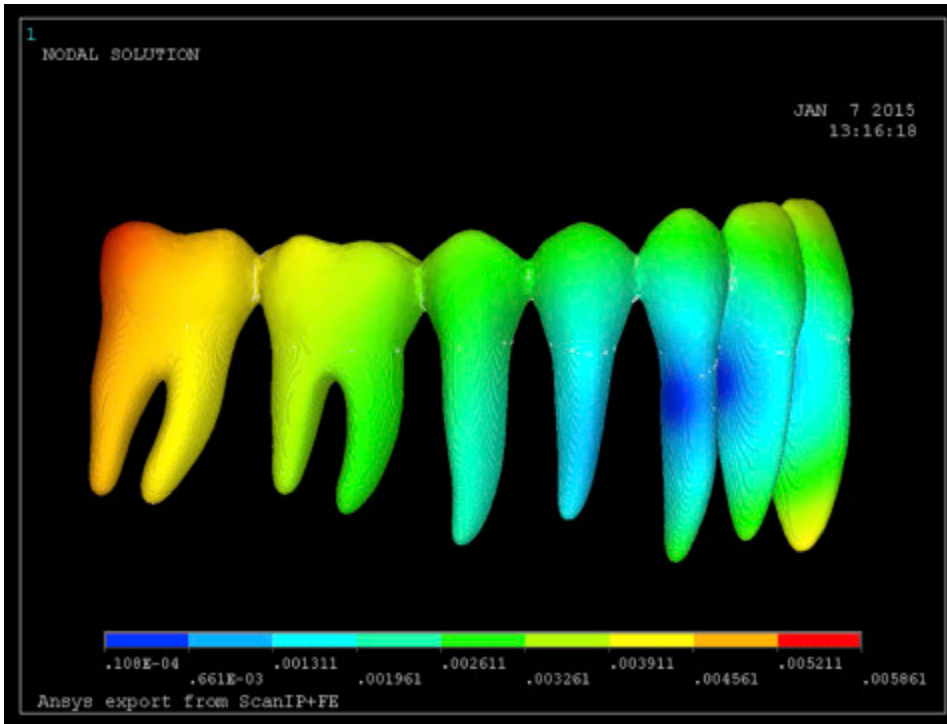
10. A skull with a near Class I occlusion is used to compare the posterior maxillary (IZC) and mandibular (MBS) anchorage sites in the same plane. The mandibular arch can be retracted as a segment by applying traction to the canine area of an archwire from bone screws inserted in two different positions: IZC and MBS mechanics are illustrated in red and blue, respectively. The lines of force (solid arrows), and their respective moments (curved arrows), are determined by the perpendicular distance (black dashed lines), relative to the center of resistance (yellow star) for the lower arch. Note that posterior mandible (PM) interradicular miniscrews deliver the same mechanics as MBS, until the roots of the molars contact the screws.



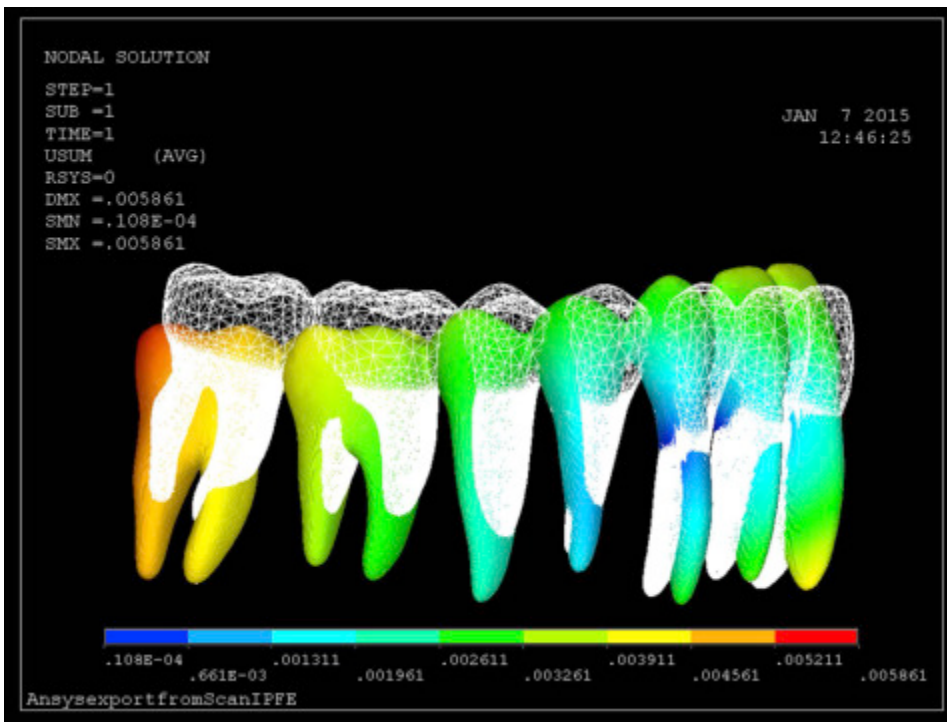
11. Cephalometric tracings document the retraction of the lower arch to correct a Class III openbite malocclusion, from the start of treatment at age 21yr (black) to the end of treatment at age 24yr (red). Bone screw anchorage in the posterior mandible and maxilla was used during treatment, but only the posterior mandibular bone screws resulted in lower molar intrusion and forward rotation of the mandible. See Shih, Lin and Roberts 2015 (reference 16) for details.



12. More detailed cephalometric tracings of the mandible are superimposed on the inferior alveolar canal and the internal symphysis. Blue is the start of treatment (21yr) and red is the finish (24yr). Note that the entire lower arch was retracted and rotated counterclockwise as a “rigid” segment. The intrusion of the molars and extrusion of the incisors reversed the etiology of the developing malocclusion documented in Figure 9.



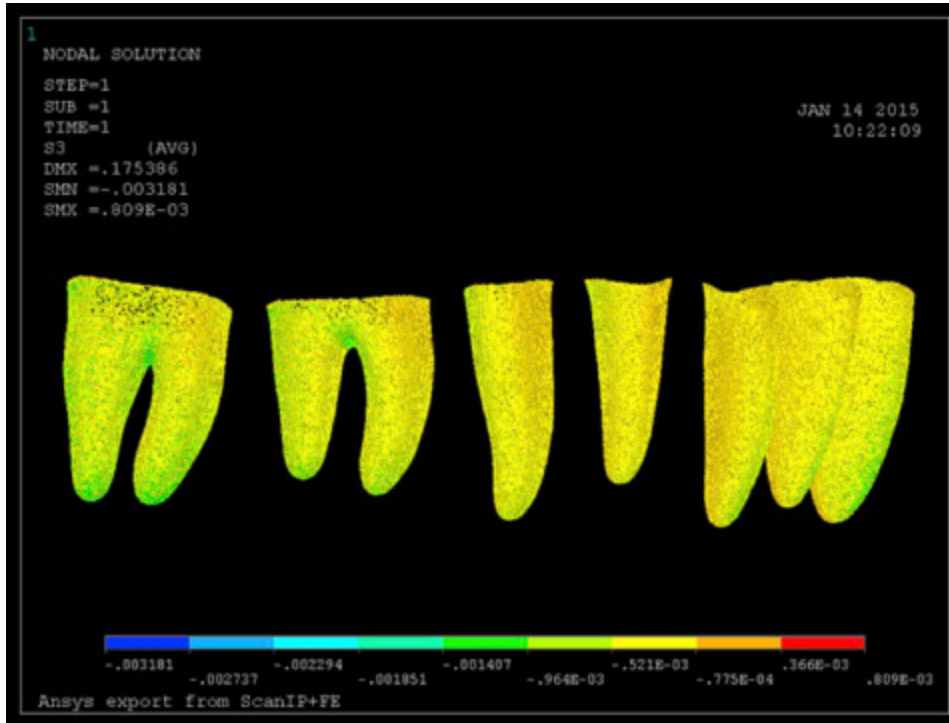
13. A retrospective FEA was used to calculate the center of rotation (blue) for lower arch retraction with determinate mechanics, as described in Shih, Lin and Roberts 2015 (reference 16). See text for details.



14. The posterior rotation of the lower arch, relative to the original position (white mesh) is determined by iterations of the FEA. Note the results are almost



identical to the actual lower arch rotation documented with cephalometrics (Figures 11 and 12).



15. PDL stress associated with the posterior rotation of the mandible appears to be <1kPa, but the error of the method suggests <5kPa is a more reliable estimate. See text for details.



Table.

Mandibular arch retraction and rotation with extra-alveolar bone screw anchorage

	Incisors		Molars		To maxill ary arch	Rotati on (°)	Treatm ent time (mo)	ABO CRE	P&W estheti cs
	AP (m m)	Vertic al (mm)	AP (m m)	Vertic al (mm)	AP (mm)				
Mean	-3.35	2.18	-4.85	-0.85	-4.88	-5.76	36.2	24.1	4.7
SD	1.55	2.51	1.78	2.22	1.41	4.77	15.3	9.5	2.1
Range	(-6 to -1)	(-6 to -1)	(-10 to -3)	(-5 to +2.5)	(-8 to -3)	(-16.5 to +3.5)	(+18 to +62)	(+11 to +37)	(+2 to +7)
Subjects (n)	17	17	17	17	17	17	16	10	6

AP, Anteroposterior; ABO CRE, American Board of Orthodontics Cast-Radiograph Evaluation; P&W esthetics, pink and white dental esthetics score.